

Lithium Insertion in Hydrogen-Containing Carbonaceous Materials

Tao Zheng, J. S. Xue, and J. R. Dahn*

Department of Physics, Simon Fraser University, Burnaby, B.C., Canada V5A 1S6

Received July 10, 1995. Revised Manuscript Received November 15, 1995⁸

Heated carbon materials were made from organic precursors between 550 and 1000 °C. High capacities for lithium were found in all of the samples heated below 800 °C, which all contain substantial hydrogen. The majority of this high capacity shows large hysteresis; that is the lithium is inserted near 0 V (versus lithium metal) and removed near 1 V. We show that the capacity exhibiting large hysteresis is proportional to the hydrogen content of the samples. We believe that lithium atoms can bind quasi-reversibly on hydrogen-terminated edges of graphene fragments in carbonaceous materials.

Introduction

It is important to maximize the specific capacity of electrode materials in order to develop high-energy density lithium-ion cells. To this end, there have recently been a number of reports^{1–5} of high-capacity carbonaceous materials whose specific capacity greatly exceeds that of graphite, 372 mAh/g. The physical mechanisms responsible for the increased capacity are currently the subject of much controversy.

Ishikawa et al.⁴ claim that lithium is filling small nanopores in what they call “pseudo isotropic carbon”, based on NMR measurements. We prepared similar hard carbons from epoxy and phenolic resins at 1000 °C.^{1,2,6,7} We believe that there is adsorption of lithium on the internal surfaces of nanopores formed by monolayer, bilayer, and trilayer graphene sheets in the hard carbons^{1,2,6,7} as schematically shown in Figure 1. Our model and Ishikawa et al.’s model are basically identical, because the pores in these materials are about 15 Å in diameter. Mabuchi et al. propose the “cavity index model” to explain the large capacity of carbons prepared at 700 °C from coal tar pitch, a soft carbon precursor.⁵ Mabuchi’s model assumes that lithium fills pores and voids in these materials, much like the models proposed above. However, the voltage profiles of the materials in refs 1, 2, 4, and 6 are radically different from those of the materials in ref 5, so it is difficult to believe that the same explanation could be true for all types of carbonaceous materials prepared at temperatures below 1000 °C.

To understand lithium intercalation in carbonaceous materials, we must consider the physics and chemistry

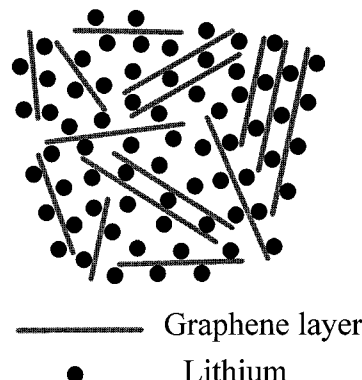


Figure 1. Adsorption of lithium on internal surfaces of nanopores formed by monolayer, bilayer, and trilayer graphene sheets in hard carbon is schematically shown.

of the structural changes that occur in the carbonaceous materials during pyrolysis.⁸ During the early stages of pyrolyzing organic precursors in inert gas (400–700 °C), organic compounds decompose, and different gases (depending on precursor composition) are released. When the heat treatment temperature is near 700 °C, the remaining carbon atoms form planar aromatic structures with predominantly hydrogen-terminated edges. Although such materials may contain other elements such as oxygen and nitrogen, carbon and hydrogen are the largest constituents on an atomic percent basis. If the organic precursors form a semi-liquid phase during pyrolysis, these planar graphene sheets can easily align in a more or less parallel fashion that finally leads to graphitization at very high heat treatment temperature (e.g., 3000 °C). Such precursors give “soft” carbons. However, if the organic precursor cross-links, a liquidlike phase is not realized during pyrolysis and the planar graphene sheets cannot align parallel to each other. These materials are hard to graphitize even at high heat-treatment temperatures and are called “hard” carbons. When the carbonaceous materials are heated to about 1000 °C, hydrogen atoms are predominantly eliminated, and the size of the

* Abstract published in *Advance ACS Abstracts*, January 1, 1996.

(1) Zheng, T.; Liu, Y.; Fuller, E. W.; Tseng, S.; von Sacken, U.; Dahn, J. R. *J. Electrochem. Soc.* **1995**, 142, 2581.

(2) Liu, Y.; Xue, J. S.; Zheng, T.; Dahn, J. R. *Carbon*, in press.

(3) Sato, K.; Noguchi, M.; Demachi, A.; Oki, N.; Endo, M. *Science* **1994**, 264, 556.

(4) Ishikawa, M.; Sonobe, N.; Chuman, H.; Iwasaki, T. 35th Battery Meeting in Japan, Nov 14–16 1994, Nagoya, paper 2B10; extended abstracts p 49. Takahashi, Y.; Oishi, J.; Miki, Y.; Yoshimura, M.; Shibahara, K.; Sakamoto, H. *Ibid.*, paper 2B05, p 39.

(5) Mabuchi, A.; Tokumitsu, K.; Fujimoto, H.; Kasuh, T. *J. Electrochem. Soc.* **1995**, 142, 1041.

(6) Zheng, T.; Zhong, Q.; Dahn, J. R. *J. Electrochem. Soc.* **1995**, 142, L211.

(7) Dahn, J. R.; Zheng, T.; Liu, Y.; Xue, J. S. *Science* **1995**, 270, 590.

(8) Several articles in *Chemistry and Physics of Carbon*; Walker, Jr., P. L., Thrower, P. A., Eds.; Marcel Dekker: New York; Vol. 1–26. For example, article by J. C. Bokpos, in Vol. 5, pp 1–118; article by E. Fizer, K. Mueller and W. Schaefer, in Vol. 7, pp 237–383; article by G. R. Millward and D. A. Jefferson, in Vol. 14, pp 1–82.

Table 1. Summary of the Samples Studied

sample	heating temp (°C)	weight percentages (%)			H/C atomic ratio (±0.03)	reversible capacity ^a (mAh/g) (±20)	irreversible capacity (mAh/g) (±20)	capacity of 1V plateau (mAh/g) (±20)
		C	H	N				
CRO550	550	93.5	3.2	0.2	0.41	880	450	570
CRO700	700	93.3	1.8	0.3	0.23	810	140	560
CRO800	800	95.1	1.3	0.3	0.16	590	180	350
CRO900	900	96.4	0.7	0.6	0.09	440	130	200
CRO1000	1000	95.5	0.3	0.5	0.04	340	100	100
KS550	550	95.1	3.2	<0.1	0.40	850	390	600
KS700	700	95.7	1.7	0.6	0.21	760	250	500
KS800	800	95.4	1.4	0.4	0.17	580	80	340
KS900	900	97.1	1.0	0.2	0.12	450	120	200
KS1000	1000	98.0	0.5	<0.1	0.06	350	60	120
PVC550	550	93.9	2.8	0.6	0.36	940	340	670
PVC700	700	94.6	1.6	0.7	0.20	770	160	500
PVC800	800	96.7	1.1	0.2	0.14	560	80	320
PVC900	900	97.9	0.7	0.4	0.09	400	70	170
PVC1000	1000	97.9	0.4	<0.1	0.05	340	80	110
OXY700	700	94.7	1.8	0.4	0.22	630	260	400
OXY800	800	95.8	0.9	0.7	0.11	540	210	230
OXY900	900	94.8	0.5	0.5	0.06	410	300	100
OXY1000	1000	97.4	0.4	1.4	0.05	560	200	80
ENR700	700	93.3	1.3	<0.1	0.17	650	680	420
ENR800	800	91.7	0.9	<0.1	0.12	610	230	280
ENR900	900	93.4	0.5	<0.1	0.06	590	170	190
ENR1000	1000	93.1	0.2	0.6	0.03	570	150	150
SUG600	600	92.5	2.3	0.1	0.30	760	380	540
SUG700	700	93.8	1.4	0.2	0.18	720	270	430
SUG800	800	95.2	0.9	0.3	0.11	620	200	300
SUG900	900	95.5	0.6	0.4	0.07	570	180	190
SUG1000	1000	97.0	0.5	0.7	0.06	530	130	130
ASUG600	600	92.9	2.4	0.2	0.31	690	490	470
ASUG700	700	91.4	1.5	0.3	0.20	580	380	330
ASUG800	800	94.3	0.9	0.3	0.12	570	220	260
ASUG900	900	95.4	0.5	0.4	0.06	600	190	170
ASUG1000	1000	97.0	0.5	0.4	0.06	560	150	120

^a Obtained from the second cycles of voltage–capacity profiles.

graphene sheets grows to 15–40 Å. In soft carbons, 3–10 of the graphene sheets are stacked in a more-or-less parallel fashion in regions called “organized carbon”.⁹ In hard carbons, the graphene sheets are not stacked in a parallel way; instead, they are arranged like a “house of cards”, shown schematically in Figure 1. Such hard carbons, therefore, have a large amount of nanoporosity.

In this paper, we show evidence that the hydrogen in carbonaceous materials heated near 700 °C plays an important role in the lithium insertion within them. Electrochemical cells were made to study the strong correlation between the hydrogen content of the samples and hysteresis in cell voltage profiles. We also studied many of the carbonaceous materials with powder X-ray diffraction, small-angle X-ray scattering (SAXS), and BET measurements. SAXS can be used to characterize the pore size distributions in carbon.¹⁰ Single-point BET surface area measurements can determine the internal surface area of open pores in the carbon. These results can help understand the structure of the carbon samples.

Experimental Section

Carbonaceous materials were prepared by pyrolysis of a variety of organic precursors at temperatures between 550 and 1000 °C.^{1,6} The precursors included Crowley pitch (CRO) obtained from the Crowley Tar Co., a petroleum pitch (KS) from Kureha Co. in Japan, poly(vinyl chloride) (PVC), an epoxy novolac resin (ENR) from Dow Chemical Co., and Oxychem

phenolic resin (OXY) from Occidental Chemical Co. The last two sample series are hard carbonaceous materials, and the others are soft. A sample of mesocarbon microbead (Osaka Gas) heat treated to 2800 °C was used as a reference for some physical parameter studies.

The carbonaceous samples were pyrolyzed in a quartz tube furnace as carefully described previously.^{1,6} Typical coin-type cells were made with lithium metal as one electrode and with a particular carbon sample as the other.¹ The electrodes of the carbonaceous materials were made by coating slurries of the carbon powder (about 90% by weight), super S carbon black (5 wt %) and PVDF dissolved in *N*-methylpyrrolidinone on copper foil substrates, using a doctor blade spreader. The electrodes were dried overnight at 110 °C in air and then pressed between flat plates at about 1000 psi pressure. Celgard #2500 separator and an electrolyte of 1 M LiPF₆ dissolved in a mixture of 30% ethylene carbonate and 70% diethyl carbonate by volume were used to construct the coin-type cells as described previously.¹ Two cells were made for each of the pyrolyzed carbonaceous materials.

The cells were tested with computer-controlled constant-current cyclers with currents stable to ±1%. The cells were placed in thermostats at 30.0 ± 0.1 °C during tests. We used currents of 18.5 mAh/g, which corresponds to C/20 based on 372 mAh/g, for the cycling tests. The irreversible capacities of the samples were determined by the difference between the first discharge (inserting lithium) and charge (removing lithium) capacities. The reversible capacities were determined from the average of the second discharge and second charge capacities. The composition of the carbonaceous samples was determined by carbon–hydrogen–nitrogen (CHN) analysis.¹ A summary of all the samples studied is given in Table 1. In addition, hard carbon samples¹¹ made from sugar (SUG) and sulfuric acid washed sugar (ASUG) are also included in Table 1.

(9) Franklin, R. E. *Proc. R. Soc.* **1951**, *A209*, 196.

(10) Foster, M. D.; Jensen, K. F. *Carbon* **1991**, *29*, 271.

(11) Xue, J. S.; Wilson, A. M.; Dahn, J. R. Canadian patent application, filed May 20, 1995.

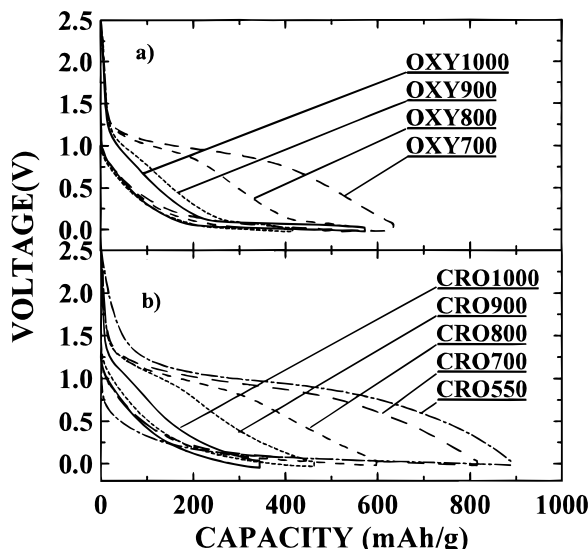


Figure 2. Voltage-capacity profiles for the second cycles of lithium/carbon cells made from (a) OXY resin and (b) CRO pitch at different temperatures as indicated.

Powder X-ray diffraction measurements were made using a Siemens D5000 diffractometer as described in refs 1 and 6. SAXS data were collected on all of the carbon samples using the same diffractometer operating in transmission mode as described in refs 2 and 6.

Single-point BET surface area measurements were made with a Micromeritics FlowSorb II 2300. A mixed gas of 70% helium and 30% nitrogen and the single-point BET equation were used.

Results and Discussion

Figure 2a shows the voltage–capacity profiles for the second cycle of lithium/carbon electrochemical cells made from OXY, a representative hard carbon, and Figure 2b shows those for samples made from CRO, a representative soft carbon. The shape of the voltage profiles for the two series of samples heated below 800 °C are similar, while they differ greatly for heating temperatures of 800 °C and above. What impressed us most is a shortening of the 1 V plateau during charge as the samples are heated above 700 °C for both the soft and hard carbons. That is, the portion of the voltage profile that displays hysteresis is removed as the samples are heated above 700 °C. The capacity of the one volt plateau (taken between 0.7 and 1.5 V for all samples) is well correlated to the hydrogen-to-carbon atomic ratio of the samples¹ as shown in Figure 3. Changing the voltage limits of the one volt plateau to other values (e.g., 0.5 and 1.5 V) does not significantly affect the correlation in Figure 3. The solid line in Figure 3 is expected if each lithium atom can bind near a hydrogen atom in the host and if a hydrogen-free carbon heated to higher than 1000 °C does not have a 1 V plateau. Mabuchi et al.'s data¹² have also been included and fit the trend well. The hydrogen contained in carbonaceous materials heated at low temperatures (below 800 °C) is important.

We have received numerous suggestions from interested scientists concerning the importance of oxygen and

(12) Mabuchi, A.; Tokumitsu, K.; Fujimoto, H.; Kasuh, T. 7th International Meeting on Lithium Batteries, May 15–20, 1994, Boston; paper I-A-10, p 207 of extended abstracts. Also see: Fujimoto, H.; Mabuchi, A.; Tokumitsu, K.; Kasuh, T. *Ibid.*, paper II-B-12, p 540.

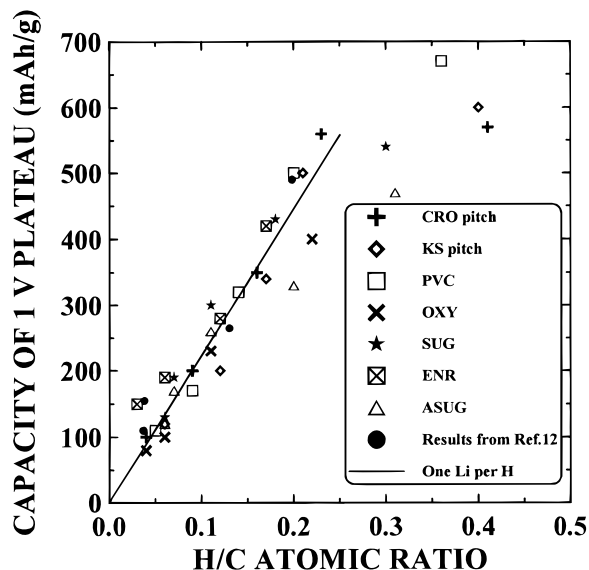


Figure 3. Capacity of the 1 V plateau measured during the second cycle of several series of samples versus the H/C atomic ratio in the samples. The solid line suggests that each lithium atom binds quasi-reversibly to one hydrogen atom.

nitrogen in the samples. Here we point out that PVC contains no nitrogen or oxygen, so neither does its pyrolyzed products. Since pyrolyzed PVC shows the same behavior in Figure 3 as the other samples, we believe the effects of oxygen and nitrogen in these materials are negligible. The presence of hydrogen is the only common factor in all these samples with a variety of microstructures prepared from a variety of precursors!

Hydrogen can affect lithium insertion in carbonaceous materials. Charge transfer from alkalis to hydrogen in carbon has been observed in ternary graphite–alkali–hydrogen materials.¹³ Furthermore, the presence of hydrogen increases the uptake of potassium in graphite from KC_8 to K_2HC_8 .¹³ One extra potassium atom per hydrogen atom can be added. In our samples, it is believed that the lithium atoms may bind on hydrogen-terminated edges of graphene fragments as discussed theoretically in ref 14. If this is true, then the capacity for the insertion of lithium should strongly depend on the hydrogen content of the carbonaceous materials as has been shown above. If the inserted lithium binds to a carbon atom which also binds a hydrogen atom, a corresponding change to the carbon–carbon bond from sp^2 to sp^3 should occur.¹⁴ Therefore, insertion and removal of lithium from hydrogen-containing carbon samples involve changes to the bonding in the host. (Normally, bonding changes in the host do not accompany intercalation and hysteresis is not observed.) Bonding changes in the host have been previously shown to cause hysteresis in electrochemical measurements like those of Figure 2.¹⁵ A conceptual model has been developed to explain the hysteresis during lithium insertion in the hydrogen-containing carbons.¹⁶

Figure 4a shows the powder X-ray patterns in the region of the (002) Bragg peak for the CRO series of

(13) Enoki, T.; Miyajima, S.; Sano, M.; Inokuchi, H. *J. Mater. Res.* **1990**, 5, 435.

(14) Papanek, P.; Radosavljevic, M.; Fischer, J. E. *Science*, submitted.

(15) Selwyn, L. S.; McKinnon, W. R.; von Sacken, U.; Jones, C. A. *Solid State Ionics* **1987**, 22, 337.

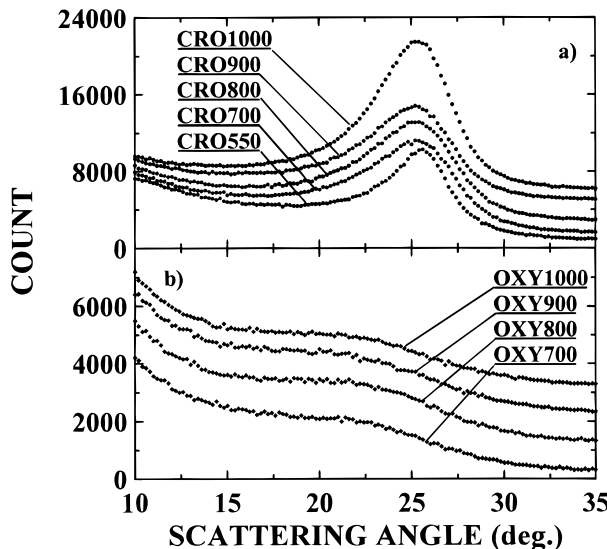


Figure 4. Powder X-ray diffraction pattern (dots) for the (002) Bragg peak of (a) CRO samples and (b) OXY samples. The data sets have been offset sequentially for clarity.

samples, and Figure 4b shows corresponding data for the OXY series. The soft carbon precursors show well-formed (002) peaks with L_c between 17 and 24 Å, suggesting that between 5 and 7 carbon layers are stacked in a more or less parallel fashion. (The Scherrer formula¹⁷ was used to determine L_c and then the number of stacked layers.) By contrast, the hard carbon samples show very poorly formed (002) peaks in Figure 4b, which indicates the presence of significant amounts of single graphene sheets as we have carefully calculated, discussed and shown in ref 2. The structure of the OXY series can be described as small graphene sheets, 20–30 Å in lateral extent⁶ (from the Scherrer formula, modified for two-dimensional peaks,¹⁷ applied to (100) and (110) peaks of the X-ray diffraction patterns⁶) arranged more or less like a “house of cards” as schematically shown in Figure 1. We expect more nanoporosity in such a structure than in the heated soft carbons with well-stacked carbon layers.

Figure 5a shows the SAXS measurements on samples CRO700, CRO1000, OXY700, and OXY1000. All these samples were measured under same conditions with the same sample mass. The Guinier formula¹⁸ was used to qualitatively model these SAXS results. The SAXS intensity, $I(q)$, from randomly located pores with homogeneous size is

$$I(q) \propto NV^2 \exp\left\{-\frac{1}{3}(qR_g)^2\right\} \quad (1)$$

where R_g is the radius of gyration of the pore, N is the number of pores, and V is their volume. A spherical pore of radius R_s has a radius of gyration R_g given by $R_g = \sqrt{\frac{3}{5}}R_s$. Materials with large pores have small angle scattering intensities which fall off rapidly with q or with scattering angle, while those with small pores show a slower decline. Materials with significant poros-

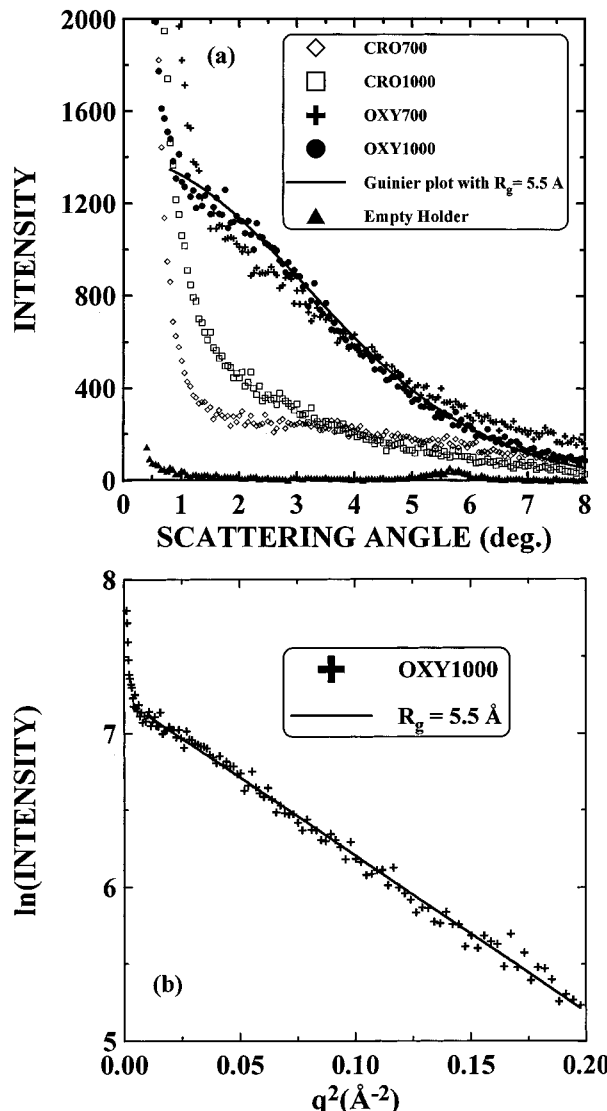


Figure 5. (a, top) Small-angle scattering intensity versus scattering angle for samples CRO700, CRO1000, OXY700, and OXY1000. The solid line is a fit using eq 1 with $R_g = 5.5$ Å which is obtained from (b). Scattering from the empty holder is included as a comparison. (b, bottom) Guinier plot for the sample OXY1000. The straight-line allows R_g to be extracted from eq 1.

ity have higher SAXS intensities, while those with less porosity show lower intensities.

Figure 5b gives $R_g = 5.5$ Å from the slope of the solid line which is the best fit to the Guinier plot of the data for sample OXY1000. Figure 5a shows that the hard carbons OXY700 and OXY1000 show evidence for significant nanoporosity, while the CRO700 and CRO1000 samples contain substantially less nanoporosity. $R_g = 5.5$ Å has been used to calculate the curve in Figure 5a, which fits the data well. This suggests that the OXY1000 sample has a relatively narrow pore size distribution with an equivalent spherical nanopore size¹⁸ of about 14 Å diameter. The mean nanopore diameters are between 12 and 14 Å for the other samples of the OXY series heated at 700, 800, and 900 °C. The high counts at very low angle ($\leq 1^\circ$) in Figure 5 are from larger pores which are typically larger than 100 Å. We found that the hard carbon samples all have significant nanoporosity, but that the soft carbon samples do not. Furthermore, samples CRO700 and CRO1000

(16) Zheng, T.; McKinnon, W. R.; Dahn, J. R.; Hysteresis During Lithium Insertion in Hydrogen-Containing Carbons. *J. Electrochem. Soc.*, submitted.

(17) Kinoshita, K. *Carbon, Electrochemical and Physicochemical Properties*, Wiley and Sons: New York, 1988.

(18) Guinier, A. *Small-Angle Scattering of X-rays*; Wiley and Sons: New York, 1955.

Table 2. Summary of Physical Properties of Selected Samples

sample	BET surface area (m ² /g)	He pychrometer density (g/cm ³)	30 tap density (g/cm ³)
OXY700	250 ± 10		0.50
OXY1000	240 ± 10		0.51
ENR700	210 ± 10	1.663	0.45
ENR1000	220 ± 10	1.852	0.60
CRO700	4.2 ± 0.2		0.66
CRO1000	4.5 ± 0.2		0.77
PVC700	24.0 ± 1.0		0.65
PVC1000	25.0 ± 1.0		0.84
KS700	7.6 ± 0.5		0.56
KS1000	7.9 ± 0.5		0.68
MCMB2800		2.162	1.26

show similar weak SAXS but completely different electrochemical behavior. This is difficult to reconcile with the "cavity index model" of Mabuchi et al., which would predict similar behavior for both.

Since SAXS measures both closed and open pores, we used the single-point BET surface area measurement to check for open pores. The results for some soft and hard carbon samples heated at 700 and 1000 °C are presented in Table 2 for comparison. The hard carbon samples studied here have about 10 times more open porosity than the soft carbons.

The "tap density" measurement is a simple way to check the bulk density of the carbon powder samples. When samples have large amounts of hydrogen or significant nanoporosity, we would expect the bulk density to be low. The 30-tap densities of some soft and hard carbon samples are listed in Table 2 compared to that of the sample MCMB2800. He pychrometer densities, obtained from ref 2, measured for samples ENR700, ENR1000, and MCMB2800 are also listed in Table 2 as a reference. The increase in He density for ENR samples heated from 700 to 1000 °C is thought to be primarily due to hydrogen loss and associated volume shrinkage. Some closed porosity (on the scale of He atoms) may still exist in the ENR1000 sample, accounting for its lower density than MCMB2800. The tap densities of the soft carbons heated at 1000 °C are consistently larger compared to the hydrogen-containing carbons and the hard carbons in Table 2. This indicates that little hydrogen and little nanoporosity can be found in the soft carbon samples heated to 1000 °C.

The results from powder X-ray diffraction, SAXS and single-point BET surface measurement are all consistent; that is, significant nanoporosity exists in the hard carbon samples but *not* in the soft carbons.

Summary

Both soft and hard carbons heated below 800 °C show large capacities which exhibit hysteresis. These materials contain substantial hydrogen. The hysteresis is eliminated when hydrogen is eliminated at higher heat-

treatment temperatures. Although the hard carbon samples show evidence for a large amount of nanoporosity, soft carbons do not. We believe that the capacity which shows large hysteresis arises from lithium atoms bound near hydrogen atoms and not from lithium adsorption within the nanopores of the materials. High-capacity carbons exhibiting large hysteresis *always* have large hydrogen content. We believe that lithium atoms can bind in the vicinity of the hydrogen atoms as discussed theoretically in ref 14.

Mabuchi et al.^{5,12} argued that large amounts of lithium can be inserted within "cavities" in hydrogen-containing carbons prepared from soft carbon. Then the chemical potential of the inserted lithium would be very close to that of metallic lithium, since inserted lithium would be only weakly bound to the carbon and cluster-type and metallike lithium would be seen. We would therefore expect the voltage of a lithium/carbon cell to be several tens of millivolts and exhibit behavior like those for hard carbons heated near 1000 °C (i.e., for OXY1000 in Figure 2). Therefore, we feel that Mabuchi's "cavity index model" may be useful for hard carbon samples without hydrogen but *certainly not* for the hydrogen-containing soft carbons for which the model was proposed.

Yata et al.¹⁹ noticed that their porous polyacenic semiconductor (PAS) materials have a large amount of hydrogen and showed a large hysteresis in the electrochemical discharging–charging process. However, they also proposed that the large capacity with hysteresis was due to the storage of lithium in the pores of the material. The principle of their idea is more or less like Mabuchi et al.'s "cavity index model".

An alternate mechanism proposed by Sato et al.³ claimed that lithium atoms can be intercalated between graphene layers to occupy nearest-neighbor sites leading to high capacity. Recent work by Nalimova et al.²⁰ has shown that this is possible only under extreme conditions of 280 °C and 50–60 kbar pressure, so it is hard to believe that it could occur under ambient conditions. Even if nearest-neighbor sites could be occupied, no hysteresis in the voltage profile would be expected, so we feel Sato's model cannot be correct.

As stated above, we believe that lithium atoms bind in the vicinity of hydrogen atoms in hydrogen-containing carbons and this is the reason for the striking correlation in Figure 3, which includes all precursors we have studied. It remains to confirm the nature of this binding both experimentally and theoretically.

CM950304Y

(19) Yata, S.; Sakurai, K.; Osaki, T.; Inoue, Y.; Yamaguchi, K. *Synth. Met.* **1990**, *38*, 185.

(20) Nalimova, V. A.; Guerard, D.; Lelaurain, M.; Fateev, O. V. *Carbon* **1995**, *33*, 177.